

# A polarization-independent torsion sensor based on the near-helical long period fiber grating

Zhihang Han (韩志行)<sup>1</sup>, Cuiting Sun (孙翠婷)<sup>1</sup>, Xiren Jin (金夕人)<sup>1</sup>, Hang Jiang (蒋航)<sup>1</sup>, Chong Yao (姚宠)<sup>1</sup>, Shuo Zhang (张硕)<sup>1</sup>, Weiliang Liu (刘卫亮)<sup>1</sup>, Tao Geng (耿涛)<sup>1,\*</sup>, Feng Peng (彭峰)<sup>2,\*\*</sup>, Weimin Sun (孙伟民)<sup>1</sup>, and Libo Yuan (苑立波)<sup>3</sup>

<sup>1</sup>College of Science, Harbin Engineering University, Harbin 150001, China

<sup>2</sup>School of Physics and Technology, University of Jinan, Jinan 250022, China

<sup>3</sup>Photonics Research Center, Guilin University of Electronics Technology, Guilin 541004, China

\*Corresponding author: gengtao\_hit\_oe@126.com; \*\*corresponding author: pengfeng8283@163.com

Received June 20, 2018; accepted August 17, 2018; posted online September 20, 2018

A torsion sensor based on the near-helical (NH) long period fiber grating (LPFG) is fabricated by using a high frequency pulsed CO<sub>2</sub> laser. Each groove of the NH-LPFG is spirally written in the four sides of a single-mode fiber. The NH-LPFG has a helical periodic vertical index modulation. This is different from the screw-type index modulation of the common helical LPFGs (H-LPFGs) fabricated in a twisted fiber. The torsion and temperature characteristics of the NH-LPFG are experimentally investigated. The temperature sensitivity is about 0.0668 nm/°C. The torsion sensitivity is 0.103 nm/(rad/m) and independent of the polarization state of incident light.

OCIS codes: 060.2430, 060.2370, 140.3470.

doi: 10.3788/COL201816.100601.

The long period fiber grating (LPFG) has attracted a great deal of attention due to the distinguishing features of low insertion loss, immunity to the electromagnetic interference, light weight, and small volume<sup>[1,2]</sup>. A variety of sensors based on the LPFG have been extensively researched, which can realize the measurement of many physical parameters, such as stain, temperature, bend, refractive index, and torsion<sup>[3-6]</sup>. Torsion is one of the most important parameters for some areas including bridges, buildings, and other engineering structures. For example, by measuring the relative displacement of different positions in a twisted cylindrical surface, an indirect measurement for the twist rate can be accomplished<sup>[7]</sup>. However, the sensor is not easy to apply in engineering due to its bulky volume. Wang *et al.* presented a small volume sensor made of a corrugated LPFG; however, it cannot discriminate the torsion direction<sup>[8]</sup>. Although the LPFGs fabricated by the CO<sub>2</sub> laser can discriminate the torsion direction and have a small volume, the torsion sensitivities are relatively lower<sup>[9]</sup>. One solution is to propose a highly sensitive directional torsion sensor, but its polarization dependence is relatively higher<sup>[10]</sup>. The other solution is to fabricate some type of helical LPFGs (H-LPFG), such as an optical fiber torsion sensor based on a chiral LPFG by twisting a two-mode fiber<sup>[11]</sup>, a paired H-LPFG with opposite helicities<sup>[12]</sup>, LPFGs written in a twisted single-mode fiber<sup>[13]</sup>, or periodically cascading a series of screw-type distortions<sup>[2]</sup>. All of these mentioned sensors based on the H-LPFG are written in the twisted fibers; however, the special H-LPFG written, respectively, in the four sides of the optical fiber has not been reported.

In this Letter, a torsion sensor based on a near-H-LPFG (NH-LPFG) structure was proposed, and both torsion and

temperature measurements were conducted. The NH-LPFG is written along a single-mode fiber via the four-side exposure method. The included angle of every two adjacent grooves is orthogonal, and every four grooves constitute a local helix grating. The torsion sensitivities in different twist rates and polarization dependences were investigated and experimentally demonstrated. The experimental results show that the proposed sensor has a good torsion direction dependence and low polarization dependence, and the torsion sensitivity is higher than that of the conventional CO<sub>2</sub> laser-induced LPFG.

The diagram of the experimental setup for the NH-LPFG fabrication is shown in Fig. 1(a). The two ends of a single-mode fiber were, respectively, fixed at two disks on a rotary platform. A high frequency pulsed CO<sub>2</sub> laser

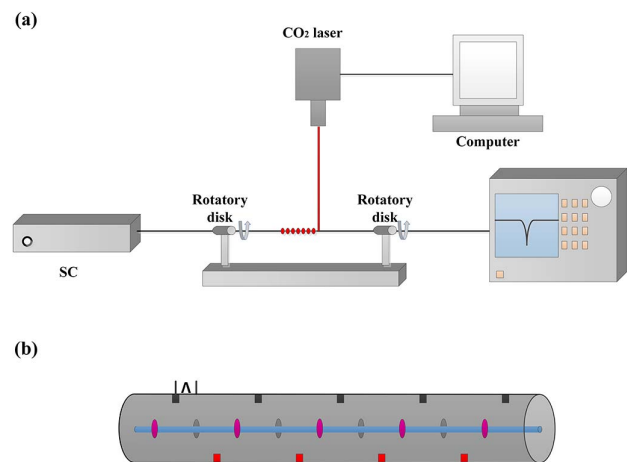


Fig. 1. (a) Experimental setup. (b) Schematic image of the NH-LPFG.

(CO<sub>2</sub>-H10, Han's Laser, including the maximum average output power of 10 W and the laser focus point diameter of 50 μm) was used to fabricate the NH-LPFG in a single-mode fiber. The transmission spectrum of the sensor is monitored by a super-continuum light source (SC) and an optical spectrum analyzer (OSA) with a range spectrum from 600 to 1700 nm.

The NH-LPFG has 48 grooves, which were marked from 1 to 48. At first, the CO<sub>2</sub> laser was used to etch 12 grooves in the single-mode fiber (including 1, 5, 9, ..., 45). Then, the two disks were rotated 90°, and another 12 grooves (including 2, 6, 10, ..., 46) were etched in the fiber. Similarly, when the two disks were rotated to 180° and 270°, two groups of 12 grooves (including 3, 7, 11, ..., 47 and 4, 8, 12, ..., 48, respectively) were etched in the fiber, respectively. This is the equivalent of the grating simultaneously fabricated by four high frequency pulsed CO<sub>2</sub> lasers in the four directions of the optical fiber. As shown in Fig. 1(b), the axial period is about 500 μm, and the total length of the NH-LPFG is about 24.5 mm.

Figure 2 shows the evolution of the transmission spectra of the NH-LPFG when the two disks were rotated from 0° to 270° with a step of 90°. The resonance wavelength of the NH-LPFG is 1645.4 nm. The phase-matching condition for NH-LPFG is similar to that of the conventional LPFG, and it can be described as

$$\lambda_{\text{res}} = (n_{\text{eff}}^{\text{co}} - n_{\text{eff}}^{\text{cl},m})\Lambda, \quad (1)$$

where  $\lambda_{\text{res}}$  is the resonant wavelength, and  $\Lambda$  is the grating period.  $n_{\text{eff}}^{\text{co}}$  and  $n_{\text{eff}}^{\text{cl},m}$  are the effective index of the fundamental core mode and the  $m$ th-order cladding mode, respectively. The cladding mode of the NH-LPFG is higher than that of conventional CO<sub>2</sub> grating by using the one-side exposure method.

Due to the conventional LPFG written by the high frequency pulsed CO<sub>2</sub> laser using the single-side exposure method, the refractive index distribution within the cross section is asymmetrical in the symmetrical optical fiber, which results in generating linear birefringence<sup>[4]</sup>. A fast axis and a slow axis are generated on the original

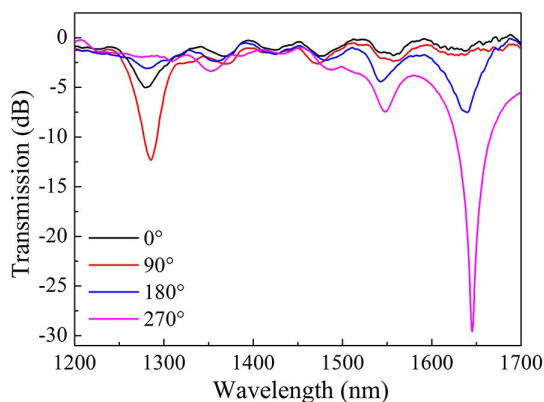


Fig. 2. Transmission spectra of the NH-LPFG under increasing rotation angles.

symmetrical optical fiber. Linearly polarized light (LP) incident along the  $x$  axis is defined as LP<sub>x</sub>, and LP incident along the  $y$  axis is defined as LP<sub>y</sub>. The optical path of LP<sub>x</sub> passing through the LPFG along the fast axis is different from that of LP<sub>y</sub> passing through the slow axis. Therefore, the spectral characteristic of the LPFG has a certain polarization dependence. The NH-LPFG can effectively reduce the asymmetrical degree of the refractive index distribution of the cross section. There is a low linear birefringence in the NH-LPFG. So, the  $x$ -axis optical path and  $y$ -axis optical path are equal after passing through the NH-LPFG. The dependence between the spectral characteristic and the polarization states can be decreased; even the NH-LPFG can have great potential as the LPFG of independent absolute polarization.

The diagram of the torsion measurement of the proposed sensor is shown in Fig. 3. The NH-LPFG was placed between a fixed disk and a rotatory disk. The distance between the two disks was 0.17 m. The polarization controller was used to control the polarization states of the input light from the SC. An OSA was used to monitor the transmission spectrum of the NH-LPFG in the torsion experiments.

The spectra of the NH-LPFG response to the torsion rate were measured without the polarization controller. The twist rate can be calculated by the following formula:  $r = \alpha/l$ , where  $\alpha$  is the turning angle of the NH-LPFG, and  $l$  is the distance between the two disks. The rotation angle varied from  $-180^\circ$  to  $180^\circ$  at  $30^\circ$  intervals; therefore, the corresponding twist rate  $r$  is applied from  $-18.3$  to  $18.3$  rad/m with a step of  $3.05$  rad/m. The transmission spectra of the NH-LPFG with different twist rates in the non-polarization state are illustrated in Fig. 4(a). It is found that the resonance wavelength (at 1645.4 nm) increases linearly towards the longer wavelength when the twist angle increases in a clockwise direction (same as the rotation direction during fabricating NH-LPFG), and the resonance wavelength has an opposite response when the twist angle increases in a counterclockwise direction. As is shown in Fig. 4(b), the torsion sensitivity of the NH-LPFG in the non-polarization state is  $0.103$  nm/(rad/m), which is higher than that of the conventional LPFG written by the CO<sub>2</sub> laser.

After the polarization controller is attached to the SC and the fixed disk, the polarization dependence between the polarization state and the torsion sensitivity can be attained.

Figure 5 shows the spectra of resonant wavelengths in both 0 and  $\pi/2$  rad polarization states, where 0 rad corresponds to the polarization state along the fast-axis

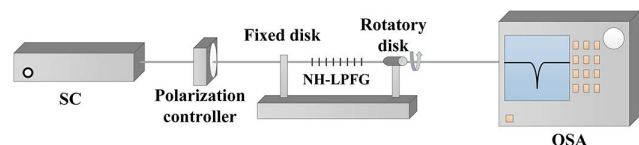


Fig. 3. Experimental setup for torsion measurement.

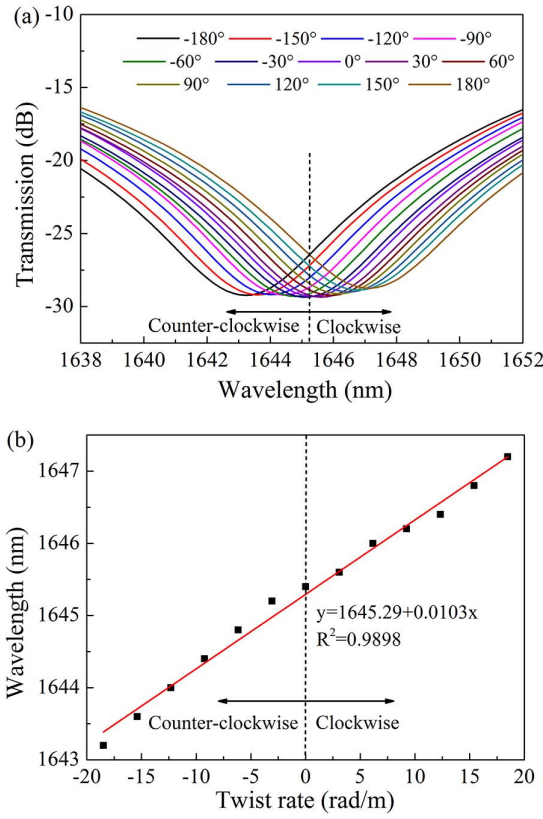


Fig. 4. (a) Transmission spectra and (b) wavelength shift of the NH-LPFG in response to the applied torsion in the non-polarization state.

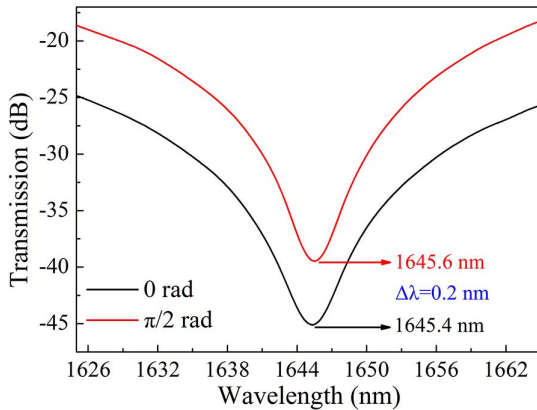


Fig. 5. Transmission spectra of the NH-LPFG in two polarization states.

direction of the fiber, and  $\pi/2$  rad corresponds to the polarization state of the slow axis. When the polarization controller is turned from 0 to  $2\pi$  rad, the maximum resonant wavelength and the minimum resonant wavelength are 1645.6 nm ( $\pi/2$  rad) and 1645.4 nm (0 rad), respectively. The resonant wavelength separation (RWS)<sup>[10]</sup> can be written as

$$\Delta\lambda_{\text{res}} = \lambda_{\text{res}}^{\text{max}} - \lambda_{\text{res}}^{\text{min}}, \quad (2)$$

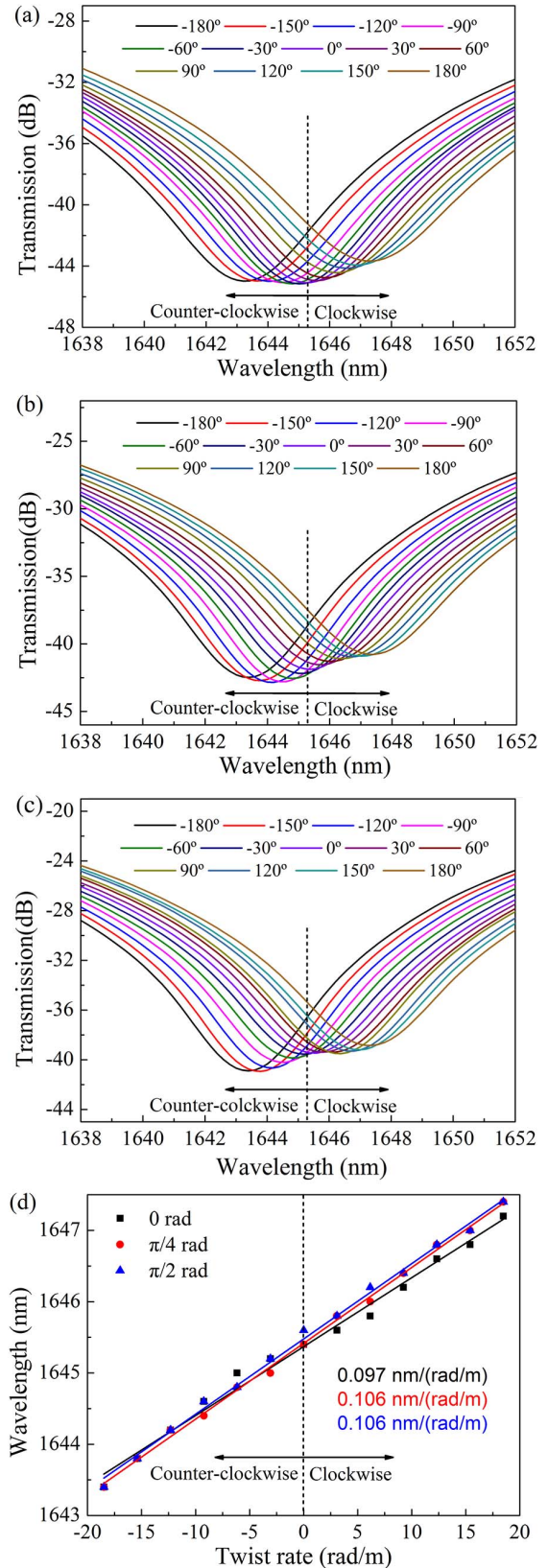


Fig. 6. Transmission spectra for the NH-LPFG in (a) 0 rad, (b)  $\pi/4$  rad, and (c)  $\pi/2$  rad polarization states under an applied torsion ranging from  $-18.3$  to  $18.3$  rad/m. (d) Wavelength shift of the NH-LPFG versus the different torsion angles in three polarization states.

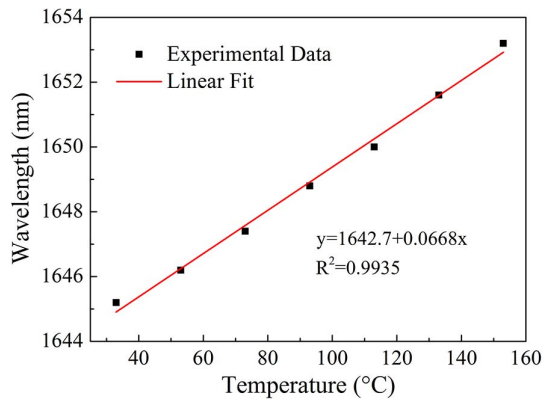


Fig. 7. Dependence of the resonance wavelength on temperature.

where  $\lambda_{\text{res}}^{\text{max}}$  is the maximum resonant wavelength, and  $\lambda_{\text{res}}^{\text{min}}$  is the minimum resonant wavelength. The RWS is 0.2 nm. Figures 6(a), 6(b) and 6(c) show the transmission spectra change with the increase of the twist rate in three polarization states, 0,  $\pi/4$ , and  $\pi/2$  rad, respectively. In these three polarization states, the resonant wavelengths have a linear red-shift in a clockwise direction, while they have a linear blue-shift in a counterclockwise direction. Figure 6(d) shows the dependence of the resonant wavelength on the twist rate in three kinds of polarization states. The three torsion sensitivities are 0.097, 0.106, and 0.106 nm/(rad/m), respectively. The torsion sensitivity of the NH-LPFG in the three polarization states is almost as large as that of the NH-LPFG in the non-polarization state. This indicates that the influence of different polarization states on the torsion sensitivity is small.

The temperature sensitivity of the NH-LPFG is experimentally investigated by changing the temperature of the heating device. When the temperature of the heating device varied from 30°C to 150°C with steps of 20°C, the resonant wavelength of the NH-LPFG has a red-shift with the increase of the temperature. The temperature sensitivity of the NH-LPFG is about 0.0668 nm/°C, as shown in Fig. 7.

A torsion sensor based on the NH-LPFG by using the high frequency pulsed CO<sub>2</sub> laser has been proposed and experimentally investigated. The NH-LPFG is the grating of the helical periodic vertical index modulation. The torsion sensitivities of the NH-LPFG have

been measured in non-polarization and three further polarization states, which are 0.103, 0.097, 0.106, and 0.106 nm/(rad/m) in the range from  $-180^\circ$  to  $180^\circ$ , respectively. They are higher than those of the conventional LPFGs by a CO<sub>2</sub> laser. The obtained RWS is 0.2 nm. The experimental results indicate that the NH-LPFG can decrease the effect between polarization states and torsion sensitivity. Furthermore, the temperature sensitivity of the NH-LPFG has also been measured as 0.0668 nm/°C. The proposed torsion sensor has a promising prospect for twist measurements.

This work was supported by the National Natural Science Foundation of China (Nos. 61377084, 41174161, and 61775044), the Joint Research Fund in Astronomy (No. U1631239) under cooperative agreement between the National Natural Science Foundation of China (NSFC) and the Chinese Academy of Sciences (CAS), and in part by the Aeronautical Science Foundation of China (No. 201608P6003).

## References

1. X. Dong, Z. Xie, Y. Song, Y. Song, K. Yin, Z. Luo, J. Duan, and C. Wang, *Opt. Laser Technol.* **97**, 248 (2017).
2. M. Deng, J. Xu, Z. Zhang, Z. Bai, S. Liu, Y. Wang, Y. Zhang, C. Liao, W. Jin, G. Peng, and Y. Wang, *Opt. Express*. **25**, 14308 (2017).
3. X. Jiang, P. Lu, Y. Sun, H. Liao, D. Liu, J. Zhang, and H. Liao, *Chin. Opt. Lett.* **16**, 040602 (2018).
4. Y. Wang, D. Richardson, G. Brambilla, X. Feng, M. Petrovich, M. Ding, and Z. Song, *Opt. Lett.* **36**, 558 (2011).
5. X. Yan, H. Fu, H. Li, and H. Qiao, *Chin. Opt. Lett.* **14**, 030603 (2016).
6. S. Guan, Q. Yu, and J. Zheng, *Chin. J. Lasers*. **37**, 1996 (2010).
7. V. Lemarquand, *IEEE Trans. Magn.* **35**, 4503 (1999).
8. L. Wang, C. Lin, and G. Chern, *Meas. Sci. Technol.* **12**, 793 (2001).
9. Y. Rao, Y. Wang, Z. Ran, and T. Zhu, *J. Lightwave Technol.* **21**, 1320 (2003).
10. C. Sun, T. Geng, J. He, A. Zhou, W. Yang, X. Jin, X. Chen, Y. Zhou, Q. Hu, and L. Yuan, *IEEE Photon. Technol. Lett.* **29**, 2179 (2017).
11. X. Cao, Y. Liu, L. Zhang, Y. Zhao, and T. Wang, *Appl. Opt.* **56**, 5167 (2017).
12. L. Xian, P. Wang, and H. Li, *Opt. Express*. **22**, 20260 (2014).
13. T. Zhu, K. Chiang, Y. Rao, C. Shi, Y. Song, and M. Liu, *J. Lightwave Technol.* **27**, 4863 (2009).
14. Y. Wang, J. Chen, and Y. Rao, *Opt. Soc. Am. J. B* **22**, 1167 (2005).